Therapeutics, Targets, and Chemical Biology

Cancer Research

Loss of Cdk2 and Cyclin A2 Impairs Cell Proliferation and Tumorigenesis

Lakshmi Gopinathan[1], Shawn Lu Wen Tan[1], V. C. Padmakumar[3], Vincenzo Coppola[3], Lino Tessarollo[3], and Philipp Kaldis[1,2]

Abstract

Cell-cycle inhibition has yet to offer a generally effective approach to cancer treatment, but a full evaluation of different combinations of cell-cycle inhibitors has not been evaluated. Cyclin A2, a core component of the cell cycle, is often aberrantly expressed in cancer where it may impact cell proliferation. In this study, we investigated the role of cyclin A2 in tumorigenesis using a conditional genetic knockout mouse model. Cyclin A2 deletion in oncogene-transformed mouse embryonic fibroblasts (MEF) suppressed tumor formation in immunocompromised mice. These findings were confirmed in mice with cyclin A2–deficient hepatocytes, where a delay in liver tumor formation was observed. Because cyclin A2 acts in complex with Cdk2 in the cell cycle, we explored a hypothesized role for Cdk2 dysregulation in this effect through conditional deletions of both genes. In oncogene-transformed MEFs lacking both genes, tumor formation was strongly suppressed in a manner associated with decreased proliferation, premature senescence, and error-prone recovery from serum deprivation after immortalization. Whereas loss of cyclin A2 led to a compensatory increase in Cdk1 activity, this did not occur with loss of both Cdk2 and cyclin A2. Our work offers a rationale to explore combinations of Cdk1 and Cdk2 inhibitors as a general approach in cancer therapy. *Cancer Res; 74(14); 3870–9. ©2014 AACR.*

Introduction

Cyclin A2 binds to and activates its catalytic partners, Cdk2 and Cdk1. Cdk/cyclin A2 complexes phosphorylate proteins like pocket proteins (Rb, p107, p130) and proteins involved in DNA synthesis, thereby driving S-phase progression (1–4). In line with its role in regulating S-phase and as a typical E2F target gene, cyclin A2 expression is induced upon entry into S-phase (1, 5), persists through the S- and G_2 phases, and is degraded upon entry into mitosis (6, 7). *In vitro* studies have postulated a role for cyclin A2 in the G_2–M phase transition (2, 8, 9). Germline cyclin A2 knockout mice die at embryonic stage E5.5, indicating an essential role for cyclin A2 in embryonic development (10). The use of conditional knockout mice has revealed that cyclin A2 is essential for cell-cycle progression of hematopoietic and embryonic stem cells but is dispensable for proliferation of mouse embryonic fibroblasts (MEF) due to the redundant functions of E-type cyclins (11).

Aberrant expression of cyclin A2 has been detected in a variety of cancers, and deregulation of cyclin A2 appears to be closely related to chromosomal instability and tumor proliferation (3, 12, 13). Cyclin A2 expression in patient tumors also appears to have prognostic value (14–19), and inhibition of cyclin A2 complexes has been shown to impair proliferation of tumor cell lines (20). Here, we developed a conditional knockout mouse model to address the *in vivo* role of cyclin A2 in cancer.

Materials and Methods

Generation of cyclin A2 conditional knockout mice

Mouse genomic DNA harboring the cyclin A2 locus was subcloned from the BAC clone RP23-297G4 (ResGen, PKB829) into the pBlight-TK vector. The locus was cloned by ligating two 4.5-kb fragments: primers 5′-CTTCATGGTCTGATGTCACA-TCGATCGATCGGGATTAGCAAAATTAAT-3′ (PKO484) and 5′-GATATCGATGCCTATGCTCATTCAAGGCATGTGAAATCC-3′ (PKO481) were used to PCR-amplify the 5′ fragment, and primers 5′-CAACCACATTTTATCACACTATCGATAGT TTGA-AAGTGTGGCTCTT-3′ (PKO485) and 5′-GAAGGTCGACAGCT-CATGAAATAGGCC AGAGAGATGGTTC-3′ (PKO483) were used for the 3′ fragment. LoxP recombination sites and a neomycin selection cassette were introduced flanking the third and fifth coding exons of the mouse cyclin A2 genomic locus using recombineering technique (21). The resulting targeting vector (PKB871; Supplementary Fig. S1A) was linearized by *Pvu*I digestion and electroporated into ES cells. Following positive

Authors' Affiliations: [1]Institute of Molecular and Cell Biology (IMCB), A*STAR (Agency for Science, Technology and Research); [2]Department of Biochemistry, National University of Singapore (NUS), Singapore, Republic of Singapore; and [3]National Cancer Institute, Mouse Cancer Genetics Program, NCI-Frederick, Frederick, Maryland

Note: Supplementary data for this article are available at Cancer Research Online (http://cancerres.aacrjournals.org/).

Current address for S.L.W. Tan: University of Cambridge, Medical Research Council Cancer Cell Unit, Hutchison/MRC Research Unit, Hills Road, Cambridge CB2 0XZ, UK; and current address for V. Coppola: The Ohio State University, Department of Molecular Virology, Immunology & Medical Genetics, 988 Biomedical Research Tower, 460 West 12th Avenue, Columbus, OH 43210.

Corresponding Author: Philipp Kaldis, Institute of Molecular and Cell Biology (IMCB), 61 Biopolis Drive, Proteos #3-09, Singapore 138673, Singapore. Phone: 65-65869854; Fax: 65-67791117; E-mail: kaldis@imcb.a-star.edu.sg

doi: 10.1158/0008-5472.CAN-13-3440

and negative selection with geneticin and ganciclovir, respectively, genomic DNA from surviving ES cell colonies was used to screen for homologous recombination by Southern hybridization (Supplementary Fig. S1B). ES cell clones (2020, 2023) that were correctly targeted were identified and used for the generation of the cyclin A2 conditional knockout mouse strain. To generate the cyclin $A2^{flox}$ allele, the neomycin cassette was removed by crossing cyclin A2 conditional knockout mice with β-actin–Flpe transgenic mice [ref. 22; strain name: B6.Cg-Tg (ACTFLPe) 9205Dym/J; stock no.: 005703; The Jackson Laboratory]. Cyclin $A2^{flox}$ mice were crossed with β-actin–Cre transgenic mice [ref. 23; strain name: FVB/N-Tg(ACTB-cre) 2Mrt/J; stock no.: 003376; The Jackson Laboratory] to obtain cyclin $A2^{WT/null}$ mice that were then intercrossed. Consistent with the embryonic lethality reported previously for cyclin A2 knockout mice (10, 11), no cyclin $A2^{-/-}$ pups were obtained (data not shown).

Isolation of primary MEFs

Isolation of primary MEFs has been described previously (24). Briefly, the head and the visceral organs of E13.5 embryos were removed, and the embryonic tissue was finely chopped using a razor blade. Following trypsinization at 37°C for 20 minutes, tissue and cell clumps were dissociated by pipetting and cells were plated in a 10-cm culture dish (passage 0). MEFs were cultured in DMEM (Invitrogen 12701-017) supplemented with 10% FCS (Invitrogen 26140) and 1% penicillin/streptomycin (Invitrogen 15140-122) at 37°C in a humidified incubator with 5% CO_2 and 3% or 21% O_2.

Cell culture and FACS analysis

Cells were stained for SA-β-galactosidase to detect senescence (25). Following knockout of cyclin A2 by addition of 4-hydroxytamaxifen (OHT) for 48 hours, MEFs were collected at various passages, seeded in 6-well dishes, and washed twice with PBS the next day. Incubation for 5 minutes in fixative solution [2%(wt/vol) formaldehyde/0.2% (wt/vol) glutaraldehyde solution in PBS] was followed by overnight incubation at 37°C in staining solution [20 mmol/L citric acid, 40 mmol/L Na_2HPO_4 (pH 6.0), 150 mmol/L NaCl, 5 mmol/L potassium ferrocyanide, 5 mmol/L potassium ferricyanide, 2 mmol/L $MgCl_2$, 1 mg/mL X-Gal (Invitrogen 15520034)]. Blue stained cells were visualized using Olympus CKX41 microscope and images were taken with an Olympus E-330 camera.

For 3T3 and proliferation assays, cyclin A2 knockout was achieved by addition of 4-OHT to MEFs for 48 hours, followed by plating 300,000 MEFs in 10-cm dishes (3T3 assay) or 1,500 cells in 5 replicates in 96-well plates (proliferation assay). In the 3T3 protocol, cells were trypsinized and counted every 3 days, followed by replating of 300,000 cells (26). For proliferation assays, cells were incubated for 4 hours in 150 μL of detection reagent [AlamarBlue (BUF012B; AbD Serotec) diluted 1:10 in growth medium]. Proliferation rates were estimated as a measure of metabolic activity by measuring fluorescence at 590 nm every 24 hours. For RO3306 experiments, confluent MEFs were serum starved in growth medium containing 0.1% serum for 72 hours, and cyclin A2 knockout was achieved concurrently by addition of 20 ng/mL 4-OHT during the starvation period. MEFs were then plated for proliferation assay in medium containing 10% serum and different concentrations of RO3306 (Calbiochem 217699).

For colony formation assays, cells were infected with the retroviral constructs LXSN-H-Ras/$p53^{DN}$ (PKB816) or LXSN-H-Ras/Myc (PKB817). Forty-eight hours after infection, 10,000 cells were plated in 10-cm dishes containing growth medium with or without 4-OHT. Colonies were visualized 6 to 8 days later by fixing cells in ice-cold methanol and staining with 0.02% Giemsa solution (Sigma GS-500). p53 inactivation was confirmed by treating infected cells with 1 μmol/L adriamycin for 24 hours and analyzing cell extracts for p53 expression.

Silencing of Cdk2 in primary liver tumor cells was performed by infection of cells with retroviral shRNA construct pMKO.1-shCdk2C (PKB824) kindly provided by Piotr Sicinski (27). This construct has been previously validated (27) and used by us in an earlier study (28).

For FACS analysis of unsynchronized MEFs, cyclin A2 knockout was induced by addition of 20 ng/mL 4-OHT (Sigma H7904) for 48 hours. For FACS analysis of synchronized MEFs, confluent MEFs were serum starved in growth medium containing 0.1% serum for 72 hours, and cyclin A2 knockout was achieved concurrently by addition of 20 ng/mL 4-OHT during the starvation period. MEFs were released into 10% serum containing medium and collected at various time points. One hour before collection of MEFs, cells were labeled with 100 μmol/L bromodeoxyuridine (BrdUrd; BD Pharmingen 550891) to monitor S-phase. Cells were trypsinized, fixed in ice-cold 70% ethanol, and stained with allophycocyanin (APC)-conjugated anti-BrdUrd antibodies (BD Pharmingen 623551) and propidium iodide (Sigma 81845). Cell-cycle analysis was performed using a FACS-Calibur flow cytometer (BD Biosciences) and FlowJo 8 software.

Western blot analysis, immunoprecipitation, and kinase assays

Lysates from MEFs were prepared as described previously (28) and used for Western blot or kinase assays. The following antibodies were used in this study: cyclin A2 (Santa Cruz Biotechnology #SC-596), cyclin B1 (Cell Signaling #4135 and #4138), cyclin E1 (eBioscience #14—6714—63), Cdk1 and Cdk2 as described (24), HSP90 (BD Biosciences #610418), p53 (Cell Signaling #2524), p21 (Santa Cruz Biotechnology #SC-6246), p27 (BD Transduction Laboratories #610242), p27 (Invitrogen #71-9600), Erk1/2 (Cell Signaling #4695), phospho-Erk1/2 (Cell Signaling #9101), actin (Santa Cruz Biotechnology #SC-1616), and c-Myc (Santa Cruz Biotechnology #SC-42). For immunoprecipitation and kinase assays, cross-linked antibodies against Cdk2 and cyclin B1 (as described in ref. 28), Cdk1 (Santa Cruz #SC-54AC), cyclin A2 (Santa Cruz #SC-751AC), cyclin B1 (Santa Cruz #SC-7393AC), and suc1 agarose beads (Millipore #14-132) were used. Kinase assays with immuno-precipitated proteins using histone H1 as substrate were performed as described previously (28).

Tumorigenesis in nude mice

Primary MEFs were transformed by infection with retroviral construct LXSN-H-Ras/$p53^{DN}$ (PKB816). Following induction

with 4-OHT for 48 hours to achieve cyclin A2 knockout, 1×10^6 MEFs in PBS were injected subcutaneously into the flanks of nude mice. Tumor measurements were taken twice a week until tumor diameters reached 20 mm, upon which mice were sacrificed. For analysis of cyclin A2 deletion in growing tumors, transformed MEFs were injected subcutaneously into the flanks of nude mice. Once tumor volumes reached 60 to 100 mm^3 (7–10 days after injection), tamoxifen pellets (Innovative Research of America, SE-361 tamoxifen-free base, 25 mg/pellet, 60-day release) were subcutaneously implanted at a site distal to the tumor. Tumor volumes (V) were calculated using this formula: $V = L \times W \times W/2$ (L, length; W, width). All procedures were done in compliance with Institutional Animal Care and Use Committee (IACUC) guidelines.

Liver tumorigenesis

Sleeping beauty transposon–induced liver tumorigenesis by hydrodynamic tail vein injections was performed as described previously (28, 29). Two- to 4-month-old mice were injected with a plasmid cocktail diluted in lactated Ringer solution through their lateral tail vein in less than 10 seconds using 27-gauge needles. The Qiagen EndoFree Plasmid Maxi kit (12362) was used for purification of plasmid DNA. About 15 μg of transposase (pGK-SleepingBeauty13) and a total of 30 μg of transposon (pT2-Caggs-NRasV12 and pT2-shRNA p53; ref. 30) encoding plasmids were injected per mouse. The injection volume corresponded to 10% of mouse body weight (i.e., 2 mL for a 20 g mouse, not exceeding 3 mL). Mice were sacrificed when moribund, which was within 3 to 4 months for control mice (those expressing cyclin A2 in their liver) and 6 to 8 months for test mice (those with cyclin A2 knockout liver), followed by histologic analysis. Ki67-positive cells in liver tumor sections were enumerated using Slidepath Digital Image Hub and TissueIA (Leica Microsystems) image analysis programs. All procedures were done in compliance with IACUC guidelines.

Results and Discussion

Delayed tumorigenesis and impaired tumor cell proliferation upon concurrent loss of Cdk2 and cyclin A2

To investigate the roles of cyclin A2 in tumorigenesis *in vivo*, we generated hepatocyte-specific cyclin A2 knockout mice and assessed the role of cyclin A2 in liver tumorigenesis. Cyclin $A2^{flox}$ mice (Supplementary Fig. S1A–S1C) were crossed to Albumin-Cre transgenic mice to specifically delete cyclin A2 in hepatocytes. Mice with hepatocyte-specific ablation of cyclin A2 (cyclin $A2^{Liv-/-}$) were viable and did not display any detectable phenotype. Histologic analysis of cyclin $A2^{Liv-/-}$ livers revealed a small increase in nuclear size (Supplementary Fig. S1E), but cyclin $A2^{Liv-/-}$ livers were otherwise indistinguishable from livers of wild-type littermates. It should be noted that the expression of Albumin-Cre begins during embryonic development but the high Cre levels required for full recombination are attained only about 3 weeks after birth, by which time liver development has been completed (31). Tumorigenesis was induced by hydrodynamic tail vein injections of activated Ras in combination with shRNA against p53 (28, 29). Liver tumors in wild-type mice could be detected as early as 2 months, and all mice examined developed tumors within 4 months. For cyclin $A2^{Liv-/-}$ mice, only 1 of 6 mice examined had developed liver tumors by 4 months, whereas the majority displayed liver tumors after 6 months (Fig. 1A and C). Phospho-Erk expression, indicative of Ras activity, could be detected in wild-type and knockout livers (Supplementary Fig. S1F) and was increased in livers with detectable tumors (2 months for wild-type and 6 months for cyclin $A2^{Liv-/-}$ livers). Cyclin A2 protein expression could be detected in wild-type liver tumors after 2 months, but no cyclin A2 was detected in cyclin $A2^{Liv-/-}$ liver tumors as expected (Supplementary Fig. S1F). Cyclin $A2^{Liv-/-}$ liver tumors expressed Cdk1 in a delayed fashion (6 months onwards, compared with 3 months for wild-type liver tumors), but no significant differences were detected in Cdk2 expression between wild-type and knockout liver tumors (Supplementary Fig. S1F). Histologic analysis of mouse livers at different time points following induction of tumorigenesis revealed a lower Ki67 index for cyclin $A2^{Liv-/-}$ livers (Fig. 1B and C), indicating impaired tumor cell proliferation in the absence of cyclin A2.

To analyze the contribution of Cdk2 in tumors lacking cyclin A2, we chose a transformed MEF model lacking both Cdk2 and cyclin A2. We crossed Cdk2 knockout mice (24) and cyclin A2 conditional knockout mice (Supplementary Fig. S1A and S1B) to Rosa26-CreERT2 mice and then intercrossed the resulting knockout strains to obtain MEFs from $Cdk2^{-/-}$cyclin $A2^{flox/flox}$Rosa26-CreERT2 embryos wherein cyclin A2 loss could be induced by the addition of 4-OHT (Supplementary Fig. S1C and S1D). Primary $Cdk2^{+/+}$cyclin $A2^{flox/flox}$Rosa26-CreERT2 or $Cdk2^{-/-}$cyclin $A2^{flox/flox}$ Rosa26-CreERT2 MEFs were transformed using activated Ras and dominant-negative p53, and cyclin A2 loss was induced with 4-OHT. Phospho-Erk expression was assessed to confirm activated Ras signaling (Supplementary Fig. S2A), and MEFs were treated with adriamycin to confirm p53 inactivation (Supplementary Fig. S2B). We analyzed the tumorigenic potential of knockout MEFs by colony formation assays and by subcutaneous transplantation into nude mice. Loss of cyclin A2 or Cdk2 resulted in fewer colonies, whereas double knockout (DKO) MEFs formed hardly any colonies; only 1 to 2 colonies per DKO plate were observed (Fig. 2A). Similar results were obtained when MEFs were transformed with activated Ras and c-Myc (Supplementary Fig. S2C and S2D). Nude mice transplanted with cyclin $A2^{flox}$ or $Cdk2^{null}$ MEFs transformed with activated Ras and dominant-negative p53 developed tumors of maximal permissible size (20 mm diameter) within 4 weeks (Fig. 2B and C). Cyclin $A2^{null}$ MEFs formed tumors with a 1- to 2-week delay when compared with cyclin $A2^{flox}$ or $Cdk2^{null}$ MEFs, whereas transformed DKO MEFs exhibited a 4-week delay in tumor formation (Fig. 2B and C). The absence of cyclin A2 in cyclin $A2^{null}$ and DKO tumors was confirmed by Western blotting and immunohistochemistry (Supplementary Fig. S2E and S2F). Thus, while the loss of Cdk2 did not affect the tumorigenic potential of transformed MEFs, loss of cyclin A2 resulted in a delay in tumor formation. However, combined loss of Cdk2 and cyclin A2 had a more severe effect, resulting

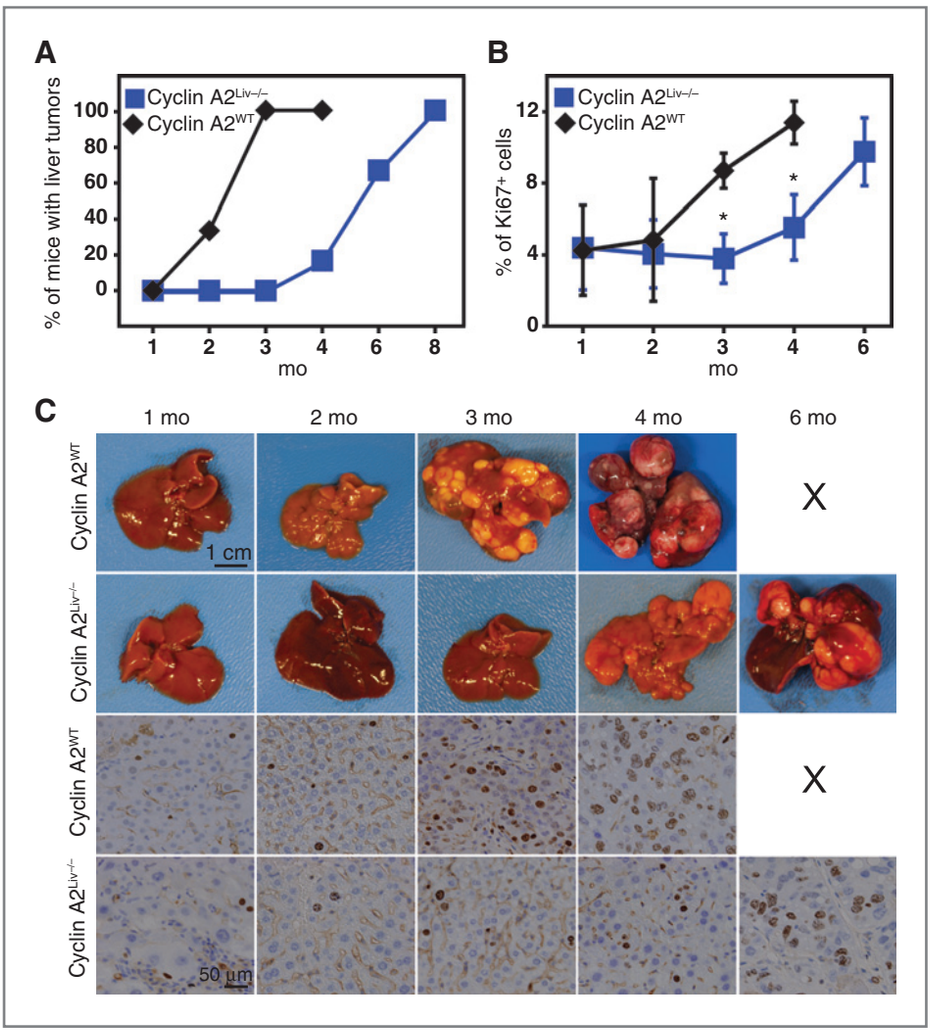

Figure 1. Delayed liver tumorigenesis in the absence of cyclin A2. Liver tumors were induced by hydrodynamic tail vein injection of Ras/shRNA p53 in wild-type (cyclin $A2^{WT}$) or liver-specific cyclin A2 knockout (cyclin $A2^{Liv-/-}$) mice. Tumor formation (assessed over 8 months) is delayed in cyclin $A2^{Liv-/-}$ mice. A and C, four to 6 mice were assessed per time point. Wild-type mice with tumors were euthanized within 4 months. X, mice with tumors did not survive for 6 months (C). B and C, cyclin $A2^{Liv-/-}$ livers display a decreased Ki67 proliferative index. *, $P < 0.05$, Student *t* test.

in significantly impaired tumorigenesis. We also assessed whether deletion of cyclin A2 in growing tumors would have an impact on tumorigenesis (Supplementary Fig. S3A and S3B). Nude mice were subcutaneously transplanted with transformed cyclin $A2^{WT}$Rosa26-CreERT2 or cyclin $A2^{flox}$ Rosa26-CreERT2 MEFs, and tumors were allowed to reach a size of 60 to 100 mm^3 (about 7–10 days after MEF allografts); following which tamoxifen pellets were subcutaneously implanted at a site distant from the tumor. While tamoxifen did not affect the growth of cyclin $A2^{WT}$ tumors (Supplementary Fig. S3B), cyclin $A2^{flox}$ tumors grew at a decreased rate in the presence of tamoxifen (Supplementary Fig. S3A). At 4 weeks following MEF transplantation, cyclin $A2^{flox}$ tumors that grew in the presence of tamoxifen displayed a 50% decrease in tumor volume. Genotyping of tumors confirmed Cre-mediated excision of cyclin A2 in the presence of tamoxifen (Supplementary Fig. S3C).

While liver tumorigenesis studies in cyclin $A2^{flox}$Albumin-Cre mice revealed a role for cyclin A2 in tumor formation (see Fig. 1), we were interested in testing cyclin A2 inhibition in a more therapeutic context. Hence, we decided to examine whether after tumor formation, inhibition of cyclin A2 (and Cdk2) could impair the proliferation of tumor cells. To this end, we induced liver tumors in cyclin $A2^{flox}$Rosa26-CreERT2 mice by tail vein injections of activated Ras in combination with shRNA against p53. Primary tumor cells were isolated for *in vitro* culture. The loss of cyclin A2 was induced by addition of 4-OHT, whereas Cdk2 knockdown was achieved using shRNA (Fig. 3A). We assessed the proliferative and colony-forming abilities of these primary liver tumor cells. In comparison to cyclin $A2^{flox}$ cells, cyclin $A2^{null}$ and shCdk2 tumor cells were similarly impaired in proliferation (Fig. 3B) and colony formation (Fig. 3C), whereas cyclin $A2^{null}$shCdk2 tumor cells exhibited the most significant impairment (Fig. 3B and C).

Concomitant loss of cyclin A2 and Cdk2 in MEFs results in impaired proliferation and premature senescence

To identify the underlying mechanisms of delayed tumorigenesis in the absence of Cdk2 and cyclin A2, we analyzed primary MEFs. In comparison to wild-type (cyclin $A2^{flox}$) MEFs, cyclin $A2^{null}$ MEFs did not display any proliferative

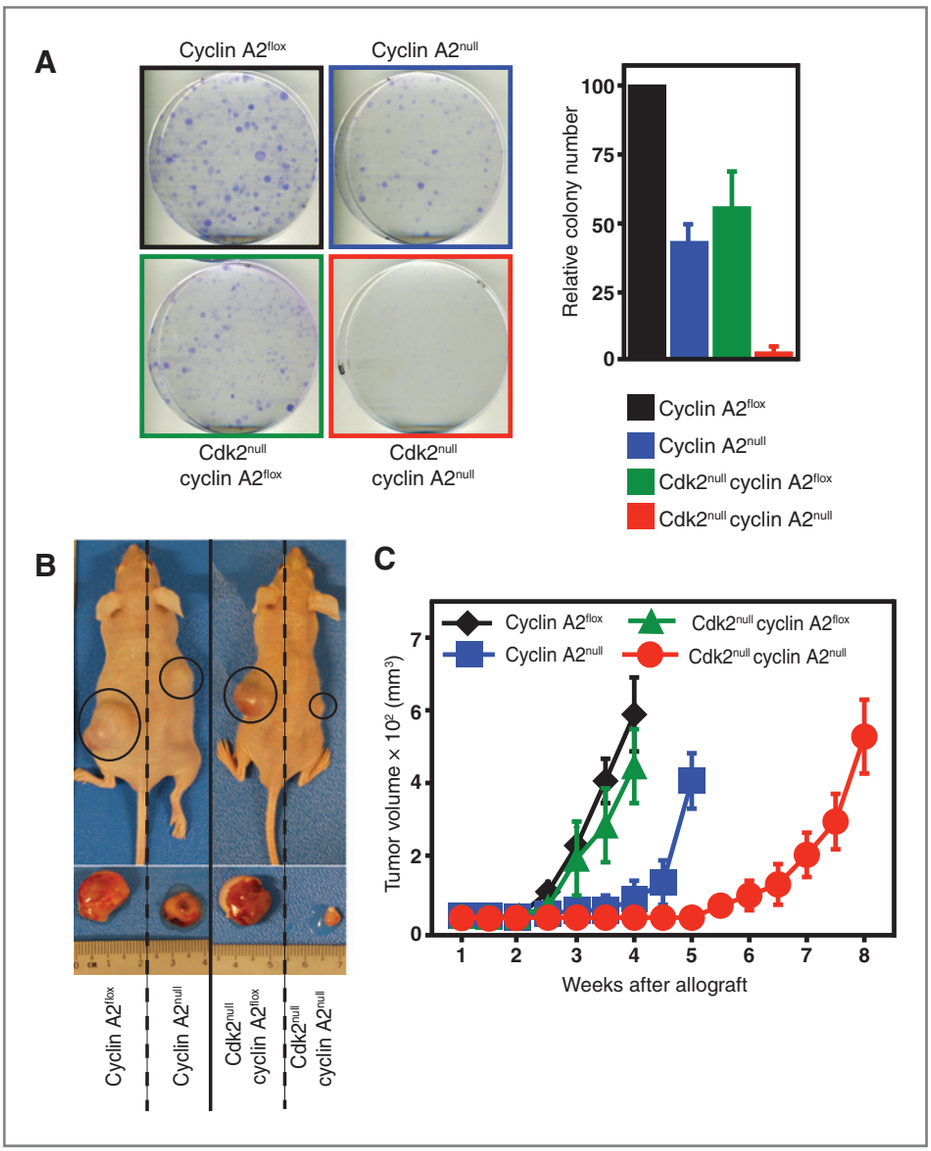

Figure 2. Transformed Cdk2^{null} cyclin A2^{null} MEFs exhibit decreased tumorigenic potential in nude mice. Cyclin A2^{flox} and Cdk2^{null}cyclin A2^{flox} MEFs were oncogenically transformed with Ras/p53^{DN} and treated with 4-OHT to induce cyclin A2 knockout. Transformed MEFs were assessed for colony formation (A) or injected subcutaneously into nude mice (B and C). Cdk2^{null}cyclin A2^{null} MEFs are resistant to transformation (A) and display decreased tumorigenic potential (B and C). Mice in B were photographed 4 weeks after MEF allografts. Data are representative of two independent MEF clones and 6 nude mice were used per genotype.

defects as described (11), whereas Cdk2^{null} MEFs displayed a small defect as has been reported previously (24, 32). In contrast, DKO MEFs displayed a significant impairment in proliferation (Fig. 4A). DKO MEFs cultures exhibited flattened morphology characteristic of senescent cells, with the percentage of β-galactosidase–positive stained cells increasing after passage 3 (Fig. 4B and Supplementary Fig. S4), indicating that the loss of Cdk2 and cyclin A2 leads to premature senescence. Analysis of the cell-cycle distribution in asynchronous MEFs using BrdUrd labeling and propidium iodide staining revealed an increase in proportion of cells in S-phase in cyclin A2^{null} MEFs, whereas DKO MEFs displayed aberrant distribution of cells with increased population of cells with 4n DNA content (Fig. 4C). In addition to cells in G_2–M, the population of cells with 4n DNA content may also represent cells that commit to endoreplication cycles, as seen by the small percentage of polyploid cells (>4n DNA content; Fig. 4C). Interestingly, the amount of polyploid cells observed in cyclin A2^{null} and DKO MEFs is substantially less compared with what we had observed in Cdk1^{null} MEFs (28). DKO MEFs entered the cell cycle normally from quiescence and also progressed through S-phase (Supplementary Fig. S5) but with a minor delay in entering S-phase that has been previously observed in Cdk2^{null} MEFs (ref. 24 and Supplementary Fig. S5] and a minor delay in exiting S-phase that was also observed in cyclin A2^{null} MEFs (Supplementary Fig. S5). This indicates that the presence of Cdk2 and cyclin A2 facilitates efficient progression through S- and G_2–M phases.

MEFs exhibit decreased immortalization rates upon loss of Cdk2 and cyclin A2

Because an essential component of oncogenic transformation is immortalization and Cdk2 in combination with cyclin A2 affected the oncogenicity of transformed MEFs (see Fig. 2),

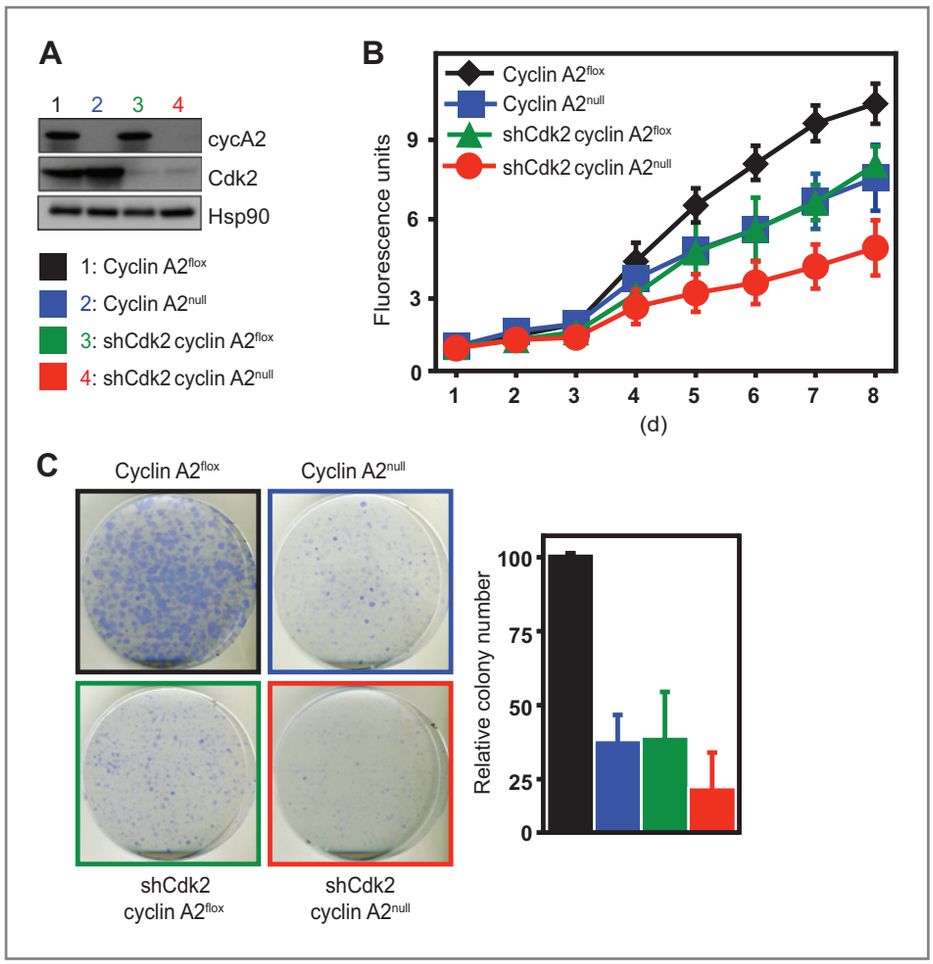

Figure 3. Impaired proliferation of primary liver tumor cells upon inhibition of cyclin A2 and Cdk2. Liver tumors were induced by tail vein injection of Ras/shRNA p53 in cyclin $A2^{flox/flox}$Rosa26-$CreERT2^{Tg/Tg}$ mice. A–C, tumors were isolated followed by dissociation and culturing of tumor cells. Cyclin A2 knockout in primary liver tumor cells was achieved by addition of 4-OHT, whereas Cdk2 was silenced by retroviral shRNA transduction (A). Cyclin $A2^{null}$ shCdk2 liver tumor cells exhibit decreased proliferation rates as determined by AlamarBlue proliferation assay (B) and resistance to colony formation (C). Data in A–C are representative of two tumor cell lines established from two mice. NPIU, normalized phosphoimager units.

we decided to investigate whether immortalization of MEFs would also be dependent on cyclin A2 and Cdk2. Therefore, we cultured MEFs under either normoxic (21% oxygen) or hypoxic (3% oxygen) conditions using a 3T3 protocol (26) to analyze the long-term proliferative potential of these cells. Both cyclin $A2^{null}$ and $Cdk2^{null}$ MEFs exhibited significantly impaired immortalization rates at early passages that were more prominent under normoxic conditions (Fig. 4D). However, while all cyclin $A2^{null}$ and $Cdk2^{null}$ clones analyzed were able to immortalize eventually, only 1 of 7 DKO clones analyzed immortalized under normoxic conditions. After an initial extended lag phase, this DKO clone eventually immortalized after approximately 30 passages (Fig. 4D, left). MEFs were analyzed during the course of 3T3 assay to confirm deletion of cyclin A2 in cyclin $A2^{null}$ and DKO MEFs (Fig. 4E). Interestingly, the expression of cyclin A2 was elevated with increasing passage in wild-type MEFs.

To fully characterize immortalized DKO MEFs, they were analyzed at passage 30 (P30). The proliferation rates for all genotypes at P30 was comparable to primary MEFs (see Fig. 4A); cyclin $A2^{null}$ MEFs displayed no proliferative defects, $Cdk2^{null}$ MEFs proliferated at a decreased rate, whereas DKO MEFs displayed the lowest proliferation rate (Supplementary Fig. S6A). Interestingly, P30 DKO MEFs were unable to survive at low-serum conditions (Supplementary Fig. S6B). While primary DKO MEFs responded appropriately to serum starvation with increased percentage of cells accumulating in G1, P30 DKO MEFs did not accumulate in G_1 (Supplementary Fig. S6C). Re-entry into the cell cycle from quiescence was largely normal for primary DKO MEFs (Supplementary Figs. S5 and S6C), whereas P30 DKO MEFs exhibited severe apoptosis and extensive polyploidy (Supplementary Fig. S6C, bottom right). While our studies suggest the importance of Cdk2 and cyclin A2 in maintaining cell-cycle fidelity in long-term cultures, we also deleted cyclin A2 at P30 in cyclin $A2^{flox}$ or $Cdk2^{null}$cyclin $A2^{flox}$ MEFs for a more direct assessment of the role of cyclin A2 in an immortalized system (Supplementary Fig. S7). Similar to the results obtained with deletion of cyclin A2 at the beginning of the 3T3 assay (see Supplementary Fig. S6C, right), deletion of cyclin A2 in P30 $Cdk2^{null}$cyclin $A2^{flox}$ MEFs resulted in apoptosis and increased polyploidy upon re-entry into the cell cycle from quiescence (Supplementary Fig. S7, bottom). It is interesting that while polyploidy in $Cdk1^{null}$ MEFs was driven by high Cdk2/cyclin A2 activity (28), the polyploidy seen here in DKO MEFs is in the absence of Cdk2 and cyclin A2. The underlying mechanism is unclear and we can only speculate that it may be based on activation of Cdc7 or other factors that induce DNA replication.

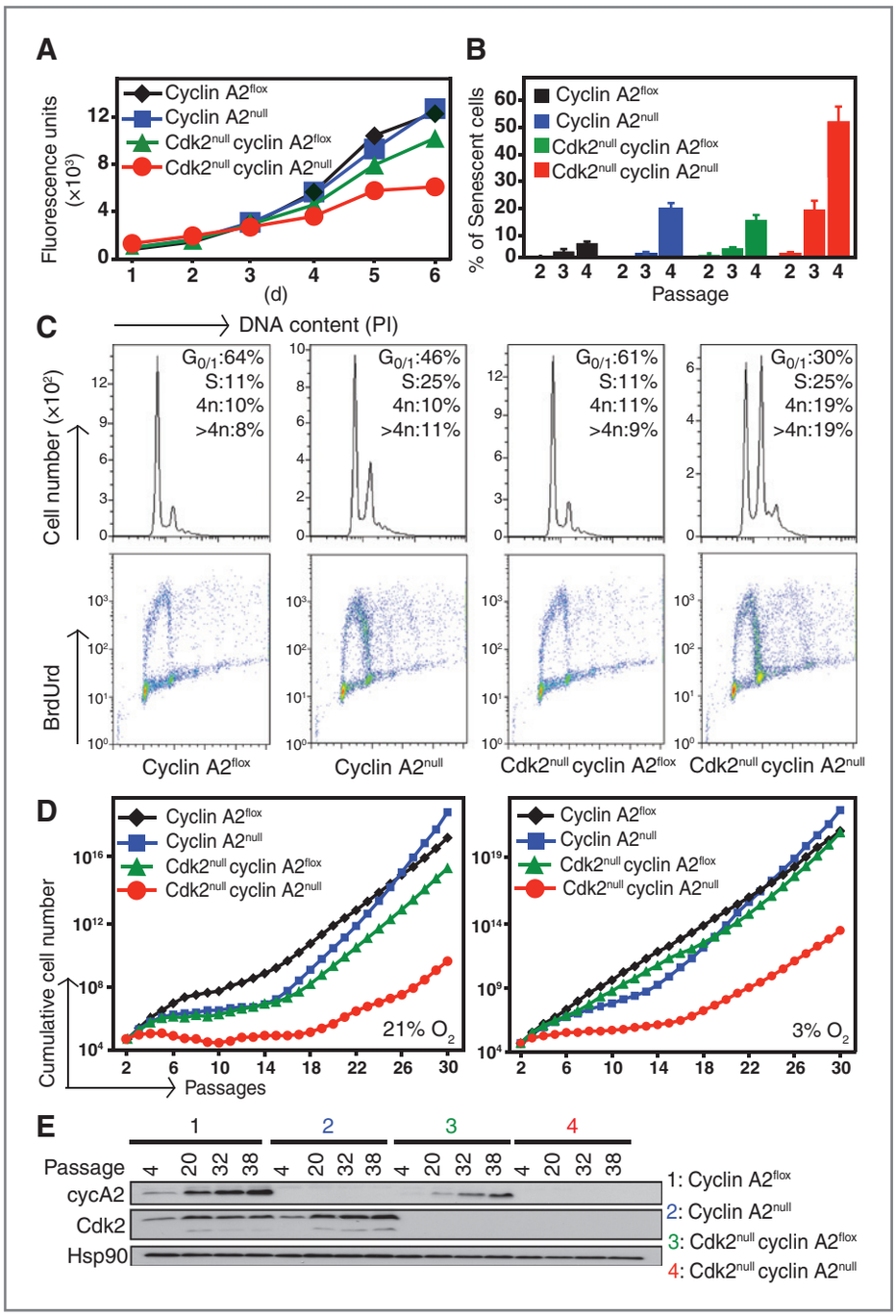

Figure 4. Concomitant loss of Cdk2 and cyclin A2 results in impaired proliferation and premature senescence. A, primary cyclin $A2^{flox}$ and $Cdk2^{null}$cyclin $A2^{flox}$ MEFs were treated with 4-OHT to induce cyclin A2 knockout, and their proliferative potential was determined by AlamarBlue proliferation assays. $Cdk2^{null}$cyclin $A2^{null}$ MEFs display impaired proliferation rates when compared with other genotypes. B, loss of cyclin A2 and Cdk2 resulted in an increased number of prematurely senescent cells in early passages, as detected by β-galactosidase staining. C, analysis of cell-cycle profile by BrdUrd labeling and propidium iodide (PI) staining revealed increased population of cells in S-phase, and cells with 4n and >4n DNA content in $Cdk2^{null}$cyclin $A2^{null}$ cells. Data are representative of three independent MEF lines. D, cyclin $A2^{flox}$ and $Cdk2^{null}$cyclin $A2^{flox}$ MEFs were treated with 4-OHT to induce cyclin A2 knockout and were cultured over several passages using a 3T3 assay at 21% (left) and 3% (right) oxygen to determine long-term propagative potential. Of 7 clones tested, only one $Cdk2^{null}$cyclin $A2^{null}$ clone survived the 3T3 assay at 21% oxygen. MEFs were collected at various passages during the course of the 3T3 assay at 21% oxygen conditions and the absence of cyclin A2 protein in cyclin $A2^{null}$ and DKO MEFs was confirmed by Western blotting of protein extracts (E).

Cdk1 kinase activity is increased upon loss of cyclin A2

The largely normal cell-cycle progression in cyclin $A2^{null}$ MEFs has been attributed to the compensatory role of cyclin E (11) and normalcy in $Cdk2^{null}$ MEFs is due to the compensatory functions of Cdk1 and Cdk4 (33–35). To understand whether these or other cell-cycle regulators were affected in primary DKO MEFs, we determined protein levels (Supplementary Fig. S8A) and kinase activity (Fig. 5A and B and Supplementary Fig. S8B) of various Cdks and cyclins at different time points following release from serum starvation. Cyclin A2 expression was ablated in cyclin $A2^{null}$ and DKO cells, whereas Cdk2 was undetectable in $Cdk2^{null}$ and DKO cells. No significant differences were detected in protein levels of other regulators such Cdk1, cyclin B1, cyclin E1, p21, and p27 (Supplementary Fig. S8A). Because cyclin E has been reported to compensate for loss of cyclin A2 in MEFs (11), we analyzed Cdk2/cyclin E complexes in cyclin $A2^{null}$ MEFs and detected increased complex formation (Supplementary Fig. S8C). In addition, we detected Cdk2/cyclin B1 complexes at low levels in cyclin $A2^{null}$ MEFs (Supplementary Fig. S8C).

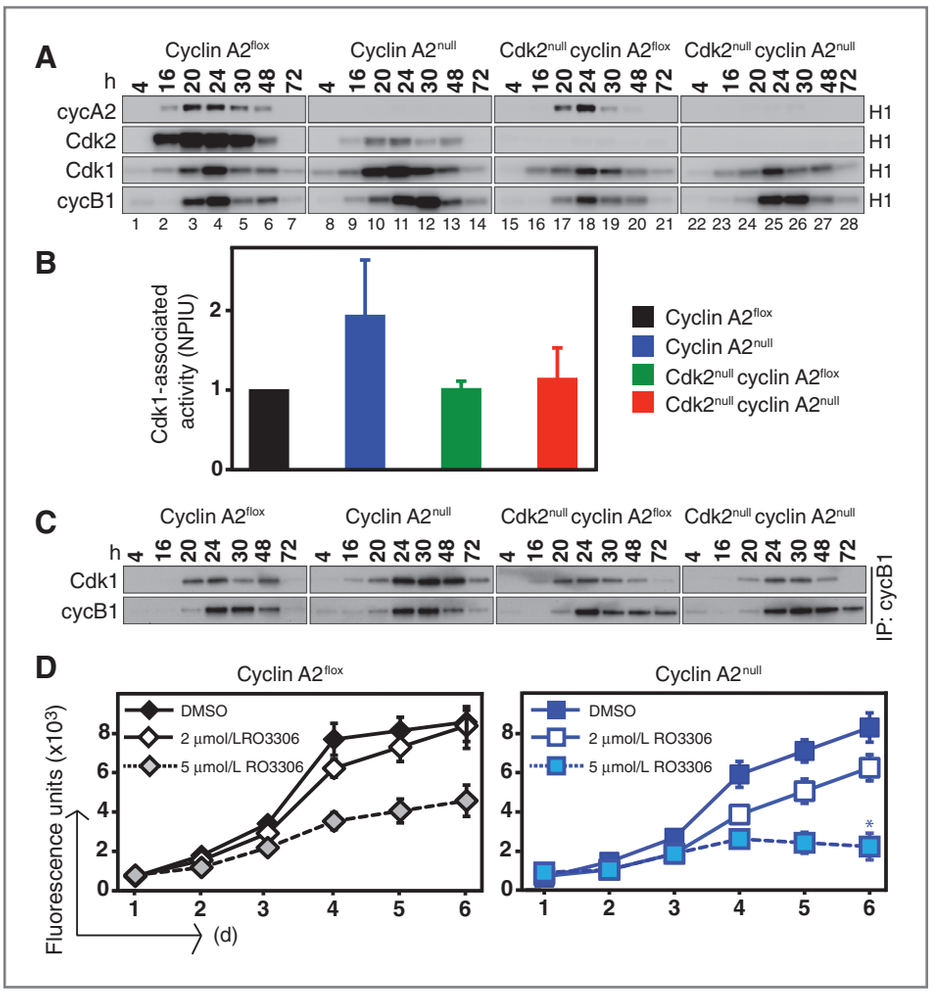

Figure 5. Activity of Cdks in primary MEFs. Primary MEFs were synchronized at G_0–G_1 by serum starvation for 72 hours and simultaneously treated with 4-OHT to induce cyclin A2 knockout. MEFs were released into S-phase by serum addition and were collected at different time points. Protein extracts were subjected to immunoprecipitation with the indicated antibodies followed by *in vitro* kinase assays using radiolabeled ATP and histone H1 as substrates. Data are representative of three independent kinase assays performed with three different MEF clones. A, quantitative analysis of Cdk1-associated activity is shown as an average of phosphoimager units for three MEF clones at 24, 30, 48, and 72 hours following serum starvation. B, the average value obtained for cyclin $A2^{flox}$ MEFs was normalized to one and values for the other genotypes were calculated comparatively. NPIU, normalized phosphoimager units. C, protein extracts were prepared from cells and subjected to coimmunoprecipitation with antibodies against cyclin B1, followed by SDS-PAGE and Western blotting with antibodies against Cdk1. Increased Cdk1/cyclin B1 complexes are detected in cyclin $A2^{null}$ MEFs but not in the other genotypes. Synchronized primary MEFs were treated with different concentrations of Cdk1 inhibitor RO3306, and their proliferative potential was determined by AlamarBlue proliferation assays. Data are representative of three independent proliferation assays performed with three different MEF clones. D, loss of cyclin A2 renders MEFs more sensitive to Cdk1 inhibition. *, $P < 0.05$, Student *t* test. Proliferative rate (slope of graphical trendline) of cyclin $A2^{null}$ MEFs is significantly lower than cyclin $A2^{flox}$ MEFs at 5 μmol/L RO3306.

The kinase activity associated with cyclin A2 was not detected in cyclin $A2^{null}$ and DKO MEFs but was slightly decreased in $Cdk2^{null}$ MEFs (Fig. 5A). Cdk2 associated activity was decreased in cyclin $A2^{null}$ (Fig. 5A, lanes 8–14, second from top) but not detectable in $Cdk2^{null}$ and DKO MEFs as expected. Importantly, Cdk1 and cyclin B1-associated kinase activities were increased in cyclin $A2^{null}$ MEFs (Fig. 5A, lanes 8–14) but remained unchanged in $Cdk2^{null}$ (Fig. 5A, lanes 15–21) and DKO MEFs (Fig. 5A, lanes 22–28). The increase in Cdk1 activity in cyclin $A2^{null}$ MEFs was statistically significant at 24-, 30-, 48-, and 72-hour time points and peaked at 30 hours following release from serum starvation, where a 2.5-fold increase was observed in comparison to cyclin $A2^{flox}$ MEFs (Supplementary Fig. S8B). The average of Cdk1-associated kinase activities at 24, 30, 48, and 72 hours following release from serum starvation is presented in Fig. 5B. There was no significant change in the protein expression of Cdk1 and cyclin B1 (see Supplementary Fig. S8A); however, elevated levels of Cdk1 were bound to cyclin B1 in cyclin $A2^{null}$ MEFs, but such an increase could not be detected in DKO MEFs (Fig. 5C). Because DKO cells exhibit a small degree of polyploidy (see Fig. 4C), it is possible that a fraction of the G_2–M cells represent cells that commit to endoreplication cycles and thereby affect the kinetics of Cdk1 activity. Nevertheless, as the overall Cdk1 activity in DKO cells

was similar to that of wild-type (cyclin $A2^{flox}$) MEFs (Fig. 5B), we assume that the small proportion of polyploid cells does not significantly confound our interpretation. Finally, a modest increase in Cdk1 activity was also observed upon loss of cyclin A2 in primary liver tumor cells (Supplementary Fig. S8E), suggesting a previously unappreciated role for Cdk1 activity in the absence of cyclin A2.

To determine the contribution of increased Cdk1 activity to the compensatory mechanisms that prevail in primary cyclin $A2^{null}$ MEFs, we used the Cdk1 inhibitor RO3306 at concentrations that could only partially inhibit Cdk1 activity and still allow for proliferation of MEFs (Fig. 5D). In comparison to control cyclin $A2^{flox}$ cells that proliferated at higher concentrations of RO3306 (5 μmol/L), loss of cyclin A2 rendered MEFs more sensitive to Cdk1 inhibition and resulted in decreased (at 2 μmol/L RO3306) or ablated proliferation (at 5 μmol/L RO3306).

Previous analysis of cyclin A2 in a conditional knockout mouse model revealed it is dispensable in MEFs but essential for proliferation of hematopoietic and embryonic stem cells. This was attributed to the role of E-type cyclins, which are expressed at sufficient levels in MEFs to compensate for absence of cyclin A2, but not in the two stem cell types studied (11). Our findings suggest that in addition to an increase in Cdk2/cyclin E complexes indicative of a compensatory role for cyclin E, there is also an increase in Cdk1 activity upon loss of cyclin A2 in MEFs. Loss of cyclin A2 rendered cells more sensitive to inhibition of Cdk1 activity using low concentrations of Cdk1-specific inhibitor RO3306. Although Cdk1 activity is unchanged in $Cdk2^{null}$ MEFs that exhibit largely normal cell-cycle dynamics (Fig. 5A and Supplementary Fig. S5; ref. 24), premature translocation of Cdk1 to the nucleus has been shown to impart near-normalcy in the absence of Cdk2 (35). We provide evidence in this study that in the absence of cyclin A2, Cdk2 activity is significantly decreased (Fig. 5A, lanes 8–14), and Cdk1 activity is increased (Fig. 5A and B). Because loss of either cyclin A2 or Cdk2 alone does not cause any overt defects, this suggests that the compensatory actions of Cdk1 that prevail in cyclin $A2^{null}$ and $Cdk2^{null}$ MEFs are impaired in DKO MEFs.

In summary, we have demonstrated functions for Cdk2 and cyclin A2 in maintaining cell-cycle fidelity and regulating tumorigenesis, which appears to be closely related to the regulation of Cdk1 activity. In addition to the loss of Cdk2/cyclin A2 complexes, deletion of cyclin A2 and Cdk2 would result in the loss of Cdk2/cyclin E and Cdk1/cyclin A2 complexes, thus affecting overall Cdk1 and Cdk2 functions. This could account for the exacerbated phenotype observed in DKO cells. We noted that administration of tamoxifen to adult cyclin $A2^{flox}$Rosa-CreERT2 mice resulted in death in around 10 days (average 10.3 ± 4.8 days; $n = 9$) that is associated with very low RBC counts. The essential functions of cyclin A2 in hematopoiesis (11) as well as our results here demonstrating proliferative defects in nontumor cells upon loss of Cdk2 and cyclin A2 complexes warrant careful design of therapy targeting cyclin A2 functions. Our results may suggest potential benefits of concurrently inhibiting Cdk1 and Cdk2 in cancer therapy.

Disclosure of Potential Conflicts of Interest

No potential conflicts of interests were disclosed..

Authors' Contributions

Conception and design: L. Gopinathan, P. Kaldis
Development of methodology: L. Gopinathan, V.C. Padmakumar
Acquisition of data (provided animals, acquired and managed patients, provided facilities, etc.): S.L.W. Tan, V. Coppola, L. Tessarollo
Analysis and interpretation of data (e.g., statistical analysis, biostatistics, computational analysis): L. Gopinathan, P. Kaldis
Writing, review, and or revision of the manuscript: L. Gopinathan, V. Coppola, L. Tessarollo, P. Kaldis
Administrative, technical, or material support (i.e., reporting or organizing data, constructing databases): P. Kaldis
Study supervision: P. Kaldis

Acknowledgments

The authors thank Zakiah Talib, June Wang, Vithya Anantaraja, and Chloe Sim for animal care; Shuhui Lim and Matias Caldez for help with nude mice experiments; Elisabeth Pfeiffenberger for help with 3T3 assays and nude mice experiments; Piotr Sicinski for reagents; Weimiao Yu for help with image analysis; and the Kaldis lab for support and discussions. They also thank the technical expertise provided by the Advanced Molecular Pathology Laboratory at IMCB. They thank Eileen Southon and Susan Reid for help in generating the cyclin $A2^{flox}$ mice, Jos Jonkers and Anton Berns for providing the Rosa26-CreERT2 mice, Mark Lewandoski for the β-actin–Cre/Flpe mice, and T. Jake Liang for the Albumin-Cre mice.

Grant Support

This work was primarily funded by the Biomedical Research Council of A*STAR (Agency for Science, Technology and Research) and partly by the Intramural Research Program of the NIH.

The costs of publication of this article were defrayed in part by the payment of page charges. This article must therefore be hereby marked *advertisement* in accordance with 18 U.S.C. Section 1734 solely to indicate this fact.

Received November 29, 2013; revised April 15, 2014; accepted April 18, 2014; published OnlineFirst May 6, 2014.

References

1. Girard F, Strausfeld U, Fernandez A, Lamb NJC. Cyclin A is required for the onset of DNA replication in mammalian fibroblasts. Cell 1991; 67:1169–79.
2. Pagano M, Pepperkok R, Verde F, Ansorge W, Draetta G. Cyclin A is required at two points in the human cell cycle. EMBO J 1992;11:961–71.
3. Yam CH, Fung TK, Poon RYC. Cyclin A in cell cycle control and cancer. Cell Mol Life Sci 2002;59:1317–26.
4. Zindy F, Lamas E, Chenivesse X, Sobczak J, Wang J, Fesquet D, et al. Cyclin A is required in S phase in normal epithelial cells. Biochem Biophys Res Commun 1992;182:1144–54.
5. Erlandsson F, Linnman C, Ekholm S, Bengtsson E, Zetterberg A. A detailed analysis of cyclin A accumulation at the G1/S border in normal and transformed cells. Exp Cell Res 2000;259: 86–95.
6. den Elzen N, Pines J. Cyclin A is destroyed in prometaphase and can delay chromosome alignment and anaphase. J Cell Biol 2001;153: 121–36.
7. Geley S, Kramer E, Gieffers C, Gannon J, Peters JM, Hunt T. Anaphase-promoting complex/cyclosome-dependent proteolysis of human cyclin A starts at the beginning of mitosis and is not subject to the spindle assembly checkpoint. J Cell Biol 2001;153: 137–48.
8. Furuno N, den Elzen N, Pines J. Human cyclin A is required for mitosis until mid prophase. J Cell Biol 1999;147:295–306.

9. Swenson KI, Farrell KM, Ruderman JV. The clam embryo protein cyclin A induces entry into M phase and the resumption of meiosis in Xenopus oocytes. Cell 1986;47:861–70.
10. Murphy M, Stinnakre MG, Senamaud-Beaufort C, Winston NJ, Sweeney C, Kubelka M, et al. Delayed early embryonic lethality following disruption of the murine cyclin A2 gene. Nat Genet 1997;15:83–6.
11. Kalaszczynska I, Geng Y, Iino T, Mizuno S, Choi Y, Kondratiuk I, et al. Cyclin A is redundant in fibroblasts but essential in hematopoietic and embryonic stem cells. Cell 2009;138:352–65.
12. Bukholm IR, Bukholm G, Nesland JM. Over-expression of cyclin A is highly associated with early relapse and reduced survival in patients with primary breast carcinomas. Int J Cancer 2001;93:283–7.
13. Malumbres M, Barbacid M. Cell cycle, CDKs and cancer: a changing paradigm. Nat Rev Cancer 2009;9:153–66.
14. Chao Y, Shih YL, Chiu JH, Chau GY, Lui WY, Yang WK, et al. Overexpression of cyclin A but not Skp 2 correlates with the tumor relapse of human hepatocellular carcinoma. Cancer Res 1998;58: 985–90.
15. Odell A, Askham J, Whibley C, Hollstein M. How to become immortal: let MEFs count the ways. Aging 2010;2:160–5.
16. Poikonen P, Sjostrom J, Amini RM, Villman K, Ahlgren J, Blomqvist C. Cyclin A as a marker for prognosis and chemotherapy response in advanced breast cancer. Br J Cancer 2005;93:515–9.
17. Volm M, Koomagi R, Mattern J, Stammler G. Cyclin A is associated with an unfavourable outcome in patients with non-small-cell lung carcinomas. Br J Cancer 1997;75:1774–8.
18. Wolowiec D, Berger F, Ffrench P, Bryon PA, Ffrench M. CDK1 and cyclin A expression is linked to cell proliferation and associated with prognosis in non-Hodgkin's lymphomas. Leuk Lymphoma 1999; 35:147–57.
19. Yasmeen A, Berdel WE, Serve H, Muller-Tidow C. E- and A-type cyclins as markers for cancer diagnosis and prognosis. Expert Rev Mol Diagn 2003;3:617–33.
20. Chen W, Lee J, Cho SY, Fine HA. Proteasome-mediated destruction of the cyclin a/cyclin-dependent kinase 2 complex suppresses tumor cell growth *in vitro* and *in vivo*. Cancer Res 2004; 64:3949–57.
21. Lee EC, Yu D, Martinez de Velasco J, Tessarollo L, Swing DA, Court DL, et al. A highly efficient *Escherichia coli*-based chromosome engineering system adapted for recombinogenic targeting and subcloning of BAC DNA. Genomics 2001;73:56–65.
22. Rodriguez CI, Buchholz F, Galloway J, Sequerra R, Kasper J, Ayala R, et al. High-efficiency deleter mice show that FLPe is an alternative to Cre-loxP. Nat Genet 2000;25:139–40.
23. Lewandoski M, Meyers EN, Martin GR. Analysis of Fgf8 gene function in vertebrate development. Cold Spring Harb Symp Quant Biol 1997;62:159–68.
24. Berthet C, Aleem E, Coppola V, Tessarollo L, Kaldis P. Cdk2 knockout mice are viable. Curr Biol 2003;13:1775–85.
25. Dimri GP, Lee X, Basile G, Acosta M, Scott G, Roskelley C, et al. A biomarker that identifies senescent human cells in culture and in aging skin *in vivo*. Proc Natl Acad Sci U S A 1995;92:9363–7.
26. Todaro GJ, Green H. Quantitative studies of the growth of mouse embryo cells in culture and their development into established lines. J Cell Biol 1963;17:299–313.
27. Kozar K, Ciemerych MA, Rebel VI, Shigematsu H, Zagozdzon A, Sicinska E, et al. Mouse development and cell proliferation in the absence of D-cyclins. Cell 2004;118:477–91.
28. Diril MK, Ratnacaram CK, Padmakumar VC, Du T, Wasser M, Coppola V, et al. Cyclin-dependent kinase 1 (Cdk1) is essential for cell division and suppression of DNA re-replication but not for liver regeneration. Proc Natl Acad Sci U S A 2012;109:3826–31.
29. Carlson CM, Frandsen JL, Kirchhof N, McIvor RS, Largaespada DA. Somatic integration of an oncogene-harboring Sleeping Beauty transposon models liver tumor development in the mouse. Proc Natl Acad Sci U S A 2005;102:17059–64.
30. Wangensteen KJ, Wilber A, Keng VW, He Z, Matise I, Wangensteen L, et al. A facile method for somatic, lifelong manipulation of multiple genes in the mouse liver. Hepatology 2008;47:1714–24.
31. Postic C, Magnuson MA. DNA excision in liver by an albumin-Cre transgene occurs progressively with age. Genesis 2000;26:149–50.
32. Ortega S, Prieto I, Odajima J, Martin A, Dubus P, Sotillo R, et al. Cyclin-dependent kinase 2 is essential for meiosis but not for mitotic cell division in mice. Nat Genet 2003;35:25–31.
33. Aleem E, Kiyokawa H, Kaldis P. Cdc2-cyclin E complexes regulate the G1/S phase transition. Nat Cell Biol 2005;7:831–6.
34. Berthet C, Klarmann KD, Hilton MB, Suh HC, Keller JR, Kiyokawa H, et al. Combined loss of Cdk2 and Cdk4 results in embryonic lethality and Rb hypophosphorylation. Dev Cell 2006;10:563–73.
35. Satyanarayana A, Hilton MB, Kaldis P. p21 inhibits Cdk1 in the absence of Cdk2 to maintain the G1/S phase DNA damage checkpoint. Mol Biol Cell 2008;19:65–77.